



## NRC Publications Archive Archives des publications du CNRC

### **The triple point of sulfur hexafluoride** Rourke, P. M. C.

This publication could be one of several versions: author's original, accepted manuscript or the publisher's version. / La version de cette publication peut être l'une des suivantes : la version prépublication de l'auteur, la version acceptée du manuscrit ou la version de l'éditeur.

For the publisher's version, please access the DOI link below. / Pour consulter la version de l'éditeur, utilisez le lien DOI ci-dessous.

#### **Publisher's version / Version de l'éditeur:**

<https://doi.org/10.1088/0026-1394/53/2/L1>

*Metrologia*, 53, 2, pp. L1-L6, 2016-03-31

#### **NRC Publications Record / Notice d'Archives des publications de CNRC:**

<https://nrc-publications.canada.ca/eng/view/object/?id=94ce3cda-5197-4a6b-9b1b-3d2848210cae>

<https://publications-cnrc.canada.ca/fra/voir/objet/?id=94ce3cda-5197-4a6b-9b1b-3d2848210cae>

Access and use of this website and the material on it are subject to the Terms and Conditions set forth at

<https://nrc-publications.canada.ca/eng/copyright>

READ THESE TERMS AND CONDITIONS CAREFULLY BEFORE USING THIS WEBSITE.

L'accès à ce site Web et l'utilisation de son contenu sont assujettis aux conditions présentées dans le site

<https://publications-cnrc.canada.ca/fra/droits>

LISEZ CES CONDITIONS ATTENTIVEMENT AVANT D'UTILISER CE SITE WEB.

**Questions?** Contact the NRC Publications Archive team at

PublicationsArchive-ArchivesPublications@nrc-cnrc.gc.ca. If you wish to email the authors directly, please see the first page of the publication for their contact information.

**Vous avez des questions?** Nous pouvons vous aider. Pour communiquer directement avec un auteur, consultez la première page de la revue dans laquelle son article a été publié afin de trouver ses coordonnées. Si vous n'arrivez pas à les repérer, communiquez avec nous à PublicationsArchive-ArchivesPublications@nrc-cnrc.gc.ca.



# The triple point of sulfur hexafluoride

**P M C Rourke**

National Research Council 1200 Montreal Road, Ottawa, ON, K1A 0R6 Canada

E-mail: [patrick.rourke@nrc-cnrc.gc.ca](mailto:patrick.rourke@nrc-cnrc.gc.ca)

**Abstract.** A cryogenic fixed point cell has been filled with high purity (99.999%) sulfur hexafluoride ( $\text{SF}_6$ ) and measured in an adiabatic closed-cycle cryostat system. Temperature measurements of the  $\text{SF}_6$  melting curve were performed using a capsule-type standard platinum resistance thermometer (CSPRT) calibrated over the International Temperature Scale of 1990 (ITS-90) subrange from the triple point of equilibrium hydrogen to the triple point of water. The measured temperatures were corrected by 0.37 mK for the effects of thermometer self-heating, and the liquidus-point temperature estimated by extrapolation to melted fraction  $F = 1$  of a simple linear regression versus melted fraction  $F$  in the range  $F = 0.53$  to 0.84. Based on this measurement, the temperature of the triple point of sulfur hexafluoride is shown to be 223.555 23(49) K ( $k = 1$ ) on the ITS-90. This value is in excellent agreement with the best prior measurements reported in the literature, but with considerably smaller uncertainty. An analysis of the detailed uncertainty budget of this measurement suggests that if the triple point of sulfur hexafluoride were to be included as a defining fixed point of the next revision of the International Temperature Scale, it could do so with a total realization uncertainty of approximately 0.43 mK, slightly larger than the realization uncertainties of the defining fixed points of the ITS-90. Since the combined standard uncertainty of this  $\text{SF}_6$  triple point temperature determination is dominated by chemical impurity effects, further research exploring gas purification techniques and the influence of specific impurity species on the  $\text{SF}_6$  triple point temperature may bring the realization uncertainty of  $\text{SF}_6$  as a fixed point material into the range of the defining fixed points of the ITS-90.

## 1. Introduction

The International Temperature Scale of 1990 (ITS-90) allows temperature to be realized using a set of defining fixed points, along with interpolating instruments and equations to smoothly interpolate between the temperatures of the fixed points [1]. In the subrange bounded by the triple points of water and equilibrium hydrogen, the ITS-90 uses platinum resistance thermometers as interpolating instruments and has eight defining fixed points: two equilibrium hydrogen vapour pressure points (near 17 K and 20.3 K), and the triple points of equilibrium hydrogen (13.8033 K), neon (24.5561 K), oxygen (54.3584 K), argon (83.8058 K), mercury (234.3156 K) and water (273.16 K) [1].

Beyond the defining fixed points of the International Temperature Scale (ITS), the Consultative Committee for Thermometry (CCT) maintains a list of so-called “secondary reference points”—fixed points that can be realized with quality near to that of the defining fixed points [2]. Improving the measurement and understanding of these secondary reference points remains a field of active research: for example, updated measurements have shown that the triple point of xenon, currently listed as a “first quality” secondary reference point [2] is suitable for inclusion as a defining fixed point of the next ITS revision [3] as a means of reducing the severity of the ITS-90 non-uniqueness problem between the triple point of argon and the triple point of water [4,5].

The triple point of sulfur hexafluoride ( $\text{SF}_6$ ) was added to the list of “second quality” secondary reference points by CCT Working Group 2 (WG2) in the 1996 list revision [2].  $\text{SF}_6$  was discovered in 1900 by Henri Moissan and Paul Lebeau [6], and has many industrial applications, most prominently as an insulating gas for high-voltage electrical power systems (see, for example, [7]). It is very stable chemically, electrically and thermally, and has been investigated extensively as a model fluid for criticality studies [8], including under weightless conditions aboard the International Space Station [9]. The triple point of  $\text{SF}_6$  has received considerably less attention than has its critical region. The handful of historical triple point determinations are summarized by Guder and Wagner [8], but the only measurement considered by CCT WG2 as worthy of inclusion in the 1996 secondary reference point list is that of Blanke *et al.*, who measured the triple point of  $\text{SF}_6$  to be 223.554(5) K [10]. More recently, Funke and coworkers reported a triple point value of 223.555(3) K [11].

Concerns about the negative health impacts of mercury have motivated the international thermal metrology community to search for a suitable alternate reference point near the triple point of mercury that could be added as a new defining fixed point of the next ITS revision. Here, a direct measurement of the triple point of  $\text{SF}_6$  on the ITS-90 is reported that demonstrates it is a higher-quality reference point than indicated by previous measurements, and, due to its proximity to the temperature of the triple point of mercury, worthy of further study as a promising candidate to be added to the next ITS revision as an alternative to mercury.

## 2. Experimental details

A set of four capsule-style standard platinum resistance thermometers (CSPRTs)—Leeds and Northrup 1876687 and 1872182, Rosemount R4794, and Chino RS143-01—were calibrated over the triple point of equilibrium hydrogen to triple point of water (“*e*-H<sub>2</sub>-TPW”) temperature range of the ITS-90. The four CSPRTs were inserted directly into the thermowells of a set of multi-thermowell sealed triple point cells [12] filled with hydrogen, neon, oxygen, argon, mercury and water, allowing simultaneous calibration of all four thermometers using the closed-cycle cryostat described in [13]. The same apparatus was used to determine the 17 K and 20.3 K points by comparison against a Tinsley rhodium-iron resistance thermometer traceable to the NRC interpolating gas thermometer realization of the ITS-90 [14]. The calibration resistance ratios  $W = R(T_{90})/R(273.16 \text{ K})$  were determined using an Automatic Systems Laboratories F18 resistance bridge combined with 25  $\Omega$  and 100  $\Omega$  Tinsley model 5685A reference resistors thermostatted in a Guildline 9732VT oil bath at 25.000(2) °C. The calibration measurements using the six ITS-90 triple point cells took place in February and June–September 2015, and the data sets thus obtained were used to determine the ITS-90 deviation function coefficients for the four CSPRTs in both the full *e*-H<sub>2</sub>-TPW subrange and the triple point of argon to triple point of water (“Ar-TPW”) subrange. The measurements and analysis presented here use the *e*-H<sub>2</sub>-TPW calibration; similar results are obtained when using the Ar-TPW calibration (see section 4.12).

In order to realize a fixed point of sulfur hexafluoride, a cylinder of “Ultra High Purity Grade” (99.999%) SF<sub>6</sub> supplied by Concorde Specialty Gases was used to fill a single-thermowell copper triple point cell (F14) of the design shown in figure 1 of [15]. The manufacturer’s analysis report for the bottle of SF<sub>6</sub> used in this study states that the only detected impurity is 9 ppm of “Air” (sum of N<sub>2</sub> + O<sub>2</sub> levels). By weighing the cell before and after filling, it was determined that the cell contained 6.225 g of SF<sub>6</sub>, which corresponds to a 0.04262 mol sample.

One of the four CSPRTs in the calibration set (Leeds and Northrup 1876687) was mounted in the thermowell of SF<sub>6</sub> cell F14, and in March 2015 an adiabatic pulsed-heating melting experiment was performed in the same apparatus as the ITS-90 calibration, using the same technique as other recent NRC cryogenic triple point determinations [3, 16, 17]. The SF<sub>6</sub> sample was cooled until it froze, and the total heat capacity of the combined cell and frozen SF<sub>6</sub> sample was measured to be 460 J K<sup>-1</sup> by observing that a 10 J heating pulse caused the cell temperature to rise by 21.8 mK in the pre-melt temperature regime between 25 and 90 mK below the SF<sub>6</sub> melt. 10 J heater pulses were then periodically applied to initiate the melt and continued until the sample had completely melted. A total heat of 225 J was required to complete the melt, corresponding to a latent heat of fusion  $\Delta H_f = 5.28 \text{ kJ mol}^{-1}$ , close to the value of 5.23 kJ mol<sup>-1</sup> calculated from the SF<sub>6</sub> entropy of fusion measurement reported by Ohta, Yamamuro and Suga [18].

### 3. SF<sub>6</sub> melting curve and triple point temperature determination

Figure 1 (a) shows the temperature of CSPRT 1876687 during the melt of the SF<sub>6</sub> sample. The CSPRT was measured using a 1 mA excitation current, except during self-heating tests when excitation currents of 1 mA then  $\sqrt{2}$  mA then 1 mA were applied in order to determine the amount of self-heating experienced by the thermometer. Four self-heating tests were performed during the SF<sub>6</sub> melt: two at approximately 57% melted fraction and two at approximately 79.5% melted fraction (not shown in figure 1). The mean self-heating found by these four tests was 0.374 mK, with a standard deviation of 0.018 mK; this self-heating correction has been subtracted from the measured temperature data, so that figure 1 shows the temperature extrapolated to 0 mA excitation current.

As seen in figure 1, each heater pulse initially causes a temperature rise in the metal shell of the fixed point cell. This is followed by a recovery period during which energy is transferred from the cell housing to the SF<sub>6</sub> sample, melting a fraction of the sample and bringing the entire cell into a new thermal equilibrium. In order to minimize the dynamic temperature-measurement error due to non-equilibrium conditions, as suggested in [19], the asymptotic equilibrium temperature,  $T_{c, \text{equ}}$ , after each pulse was found by modelling the thermal recovery period following each pulse by a superposition of exponential components. All of the thermal recovery periods for the melt shown in figure 1 were well-described by a model with two exponential components: one for the dominant, fast energy-transfer process between the metallic cell body and the adjacent portions of the SF<sub>6</sub> sample, and another for slower, more subtle equilibration processes within the sample and cell [19]. Each thermal recovery period was fitted separately from the others, to allow for changes in the thermal behaviour of the cell and sample as a function of melted fraction, and the resulting exponential fits to the experimental data are shown in figure 1 (b).

The internal thermal resistance between the metallic body of the cell and the solid phase of the sample,  $R_{cs}$ , was determined after each heater pulse  $i$  from the exponential fit characterizing the energy transfer from the cell body to the SF<sub>6</sub> sample as  $R_{cs, i} = C_{\text{cell}} \tau_{1, i}$ , where  $C_{\text{cell}}$  is the total heat capacity of the metallic parts of the cell only (460 J K<sup>-1</sup> from section 2 minus the 5 J K<sup>-1</sup> total heat capacity of the completely frozen SF<sub>6</sub> sample, calculated using the specific heat of solid SF<sub>6</sub> from [18]), and  $\tau_{1, i}$  is the fitted time constant of the dominant exponential component modelling the thermal recovery period after heater pulse  $i$ . The mean value of  $R_{cs}$  over the first 20 heater pulses in the melt is 0.42 K W<sup>-1</sup>, with standard deviation 0.08 K W<sup>-1</sup>.  $R_{cs}$  increases rapidly over the final three pulses, reaching a value of 1.6 K W<sup>-1</sup> after pulse 23, due to the little remaining mass of solid SF<sub>6</sub> in this regime being in relatively poor thermal contact with the cell body.

Figure 2 plots the temperature versus melted fraction for the SF<sub>6</sub> melt shown in figure 1, with the open symbols representing the asymptotic equilibrium temperatures,  $T_{c, \text{equ}}$ , obtained from the exponential fits to the self-heating-corrected CSPRT 1876687 data shown in figure 1 (b). A simple linear regression versus melted fraction  $F$  was performed using data from the flat part of the melt plateau, from  $F = 0.53$  to  $F = 0.84$  (pulses 13 to 20).  $T_{c, \text{equ}}$  data from the final three pulses have been excluded from the fit due to the high  $R_{cs}$  for these pulses, as

determined above. The resulting fit, extrapolated to  $F = 1$ , is shown as a solid line in figure 2, and has a fitted slope of  $1.55(22) \times 10^{-4}$  K and fitted  $F = 0$  intercept of 223.555 074(16) K. By extrapolating this fit to the liquidus point at  $F = 1$ , the liquidus-point temperature is estimated to be 223.555 228 K, with a fitting uncertainty of 27  $\mu$ K.

Thus, the best estimate of the SF<sub>6</sub> triple point, based on the liquidus-point temperature obtained from a simple linear regression versus melted fraction  $F$  of a melt plateau of a Concorde Specialty Gases sample, is  $T_{\text{tp}} = 223.555\ 23$  K.

## 4. Uncertainty budget

### 4.1. Chemical impurities

A 410  $\mu$ K uncertainty contribution arising from the chemical impurities present in the sulfur hexafluoride sample is the dominant uncertainty component for the present determination of the triple point of SF<sub>6</sub>. This uncertainty component is estimated in an Overall Maximum Estimate (“OME”) approach as [20]

$$\delta T_{\text{impurity}} = \frac{1}{\sqrt{3}} \left( \frac{c_{11}}{A} \right) \quad (1)$$

where  $c_{11} = 9$  ppm is the impurity concentration when the fixed-point material is completely melted ( $F = 1$ ), taken from the manufacturer’s analysis report described in section 2 for the bottle of SF<sub>6</sub> used in this study, and  $A = \Delta H_f / RT_{\text{tp}}^2$  is the first cryoscopic constant. Using the measured latent heat of fusion  $\Delta H_f = 5.28$  kJ mol<sup>-1</sup> from section 2, measured triple point temperature  $T_{\text{tp}} = 223.555\ 23$  K from section 3, and molar gas constant  $R = 8.314\ 4598$  J mol<sup>-1</sup> K<sup>-1</sup> from CODATA [21], the first cryoscopic constant of SF<sub>6</sub> is calculated to be  $A = 0.0127$  K<sup>-1</sup>, indicating that the liquidus point of SF<sub>6</sub> should be depressed by 79  $\mu$ K per part per million (ppm) of impurity.

### 4.2. Propagated calibration uncertainty

Table 1 shows the NRC standard realization uncertainties of the ITS-90 defining fixed points [3] (with the exception of the triple point of water, which is treated separately below)—uncertainties which are an unavoidable part of realizing the ITS-90, and in line with those of other national metrology institutes [22]—along with the values of these uncertainty contributions when propagated to 223.555 23 K. When added in quadrature, only the mercury triple point uncertainty contributes meaningfully to the combined propagated calibration uncertainty, yielding a 232  $\mu$ K uncertainty component on the triple point temperature of SF<sub>6</sub>.

### 4.3. Uncertainty propagated from the TPW

An 80  $\mu$ K uncertainty component propagated to the triple point of SF<sub>6</sub> from the triple point of water (TPW) is calculated as a product of the TPW realization uncertainty for CSPRTs (100  $\mu$ K) and the nominal resistance ratio at the triple point of SF<sub>6</sub>:  $W = R(223.555\ 23\ \text{K}) / R(273.16\ \text{K}) \approx 0.8$ .

#### 4.4. Hydrostatic pressure

A 76  $\mu\text{K}$  uncertainty due to hydrostatic pressure is calculated as

$$\delta T_{\text{pressure}} = \frac{h_{\text{liquid}}}{2} \rho_{\text{liquid}} g \left( \frac{\partial T_{\text{tp}}}{\partial p} \right) \quad (2)$$

where  $h_{\text{liquid}} = 13.1$  mm is the calculated height of the  $\text{SF}_6$  liquid surface within the cell;  $\rho_{\text{liquid}}$  is the  $\text{SF}_6$  liquid density, extrapolated to the  $\text{SF}_6$  triple point [8];  $g$  is the acceleration due to gravity; and  $(\partial T_{\text{tp}}/\partial p)$  is the pressure coefficient of the  $\text{SF}_6$  triple point temperature.  $(\partial T_{\text{tp}}/\partial p)$  is estimated as  $6.4 \times 10^{-7}$   $\text{K Pa}^{-1}$  using the Clausius-Clapeyron relation, measured latent heat of fusion  $\Delta H_f$  from section 2, measured triple point temperature  $T_{\text{tp}}$  from section 3,  $\text{SF}_6$  liquid density extrapolated to the  $\text{SF}_6$  triple point [8], and  $\text{SF}_6$  solid density extrapolated to the  $\text{SF}_6$  triple point [23].

#### 4.5. CSPRT Type 3 non-uniqueness

One of the mathematical ambiguities of the ITS-90 is the Type 3 non-uniqueness of calibrated platinum resistance thermometers: temperature measurements made with several different thermometers agree with one another, by definition, at the ITS-90 defining fixed points, but disagree with one another at temperatures between the defining fixed points [4,5]. Expressions for the uncertainty due to Type 3 non-uniqueness are derived in table 7.2 of reference [24] by fitting the temperature-dependent standard deviation of a set of many thermometers from the comprehensive experimental data of reference [5] in temperature intervals between 24 K and 273.16 K. In the temperature range 83.8058 K to 234.3156 K, the uncertainty due to Type 3 non-uniqueness is estimated as [24]

$$\delta T_{\text{non-uniqueness}} = 2.2 \times 10^{-4} (T - 83.8058)^{0.75} (234.3156 - T)^{0.75} \quad (3)$$

where  $\delta T_{\text{non-uniqueness}}$  is in units of mK for  $T$  expressed in units of K. For  $T = 223.555$  23 K,  $\delta T_{\text{non-uniqueness}} = 0.053$  mK = 53  $\mu\text{K}$ .

#### 4.6. Determination of fixed point value

A 27  $\mu\text{K}$  uncertainty in determining the fixed-point value comes from the fitting uncertainty of the liquidus-point temperature estimated from the extrapolation to  $F = 1$  of the linear fit versus melted fraction  $F$  to the experimental data shown in figure 2, as described in section 3; it is a measure of the scatter and non-linearity in the fitted data over the 0.53 to 0.84 melted fraction fitting range.

#### 4.7. Static temperature measurement

A 22  $\mu\text{K}$  static temperature-measurement uncertainty due to stray heat flux (non-adiabaticity of the apparatus), caused by imperfect balance of the control set points of the various shields within the cryostat, is estimated as [19]

$$\delta T_{\text{stat}} = \frac{R_{\text{cs}}}{R_{\text{e}}} |\Delta T_{\text{e}}| \quad (4)$$

where  $R_{cs}$  is the internal thermal resistance between the metallic body of the cell and the solid phase of the sample,  $R_e$  is the total thermal isolation resistance between the cell and its environment, and  $\Delta T_e$  is the temperature offset of the environment relative to the perfect adiabatic condition. The mean value of  $R_{cs} = 0.42 \text{ K W}^{-1}$  over the first 20 heater pulses from section 3 was used, since the final three pulses were excluded from the fit used to obtain the liquidus-point temperature.  $R_e = 94 \text{ K W}^{-1}$  was determined by observing the effect of different  $T_e$  offsets on the temperature drift rate of the  $\text{SF}_6$  cell in the pre-melt regime between 25 and 90 mK below the  $\text{SF}_6$  melt, taking into account the  $460 \text{ J K}^{-1}$  total heat capacity of the combined cell and frozen  $\text{SF}_6$  sample from section 2.  $|\Delta T_e| = 4.9 \text{ mK}$  was determined immediately following the  $\text{SF}_6$  melt by letting the cell temperature drift for 29 hours under the same environmental conditions as during the melt, and fitting the resulting curve to a single exponential decay function.

#### 4.8. CSPRT self-heating correction, accuracy of resistance bridge ratio, and standard resistors

An  $18 \mu\text{K}$  uncertainty due to the CSPRT self-heating correction is the standard deviation of the four self-heating tests of CSPRT 1876687 described in section 3. A  $13 \mu\text{K}$  uncertainty due to the accuracy of the F18 resistance bridge assumes a ratio uncertainty of  $5 \times 10^{-8}$  full scale, as claimed by the manufacturer and supported by in-house characterization using an Automatic Systems Laboratories ratio test unit and an Aeonz resistance bridge calibrator. A  $2 \mu\text{K}$  uncertainty associated with the stability of the standard resistors is derived from an assumed temperature coefficient of  $3 \text{ ppm } ^\circ\text{C}^{-1}$  and a resistor bath stability of  $2 \text{ m}^\circ\text{C}$ .

#### 4.9. Dynamic temperature measurement

A  $1 \mu\text{K}$  dynamic temperature-measurement uncertainty is the mean fitting uncertainty of the  $T_{c,\text{equ}}$  values from the exponential fits shown in figure 1 (b), in the 0.53–0.84 melted fraction range (the range used for the simple linear regression versus melted fraction in section 3).

#### 4.10. Isotopic composition

Since  $\text{SF}_6$  is a heavy molecule whose majority component, fluorine, is a monoisotopic element, variations in isotopic composition are expected to have little effect on the triple point temperature. Notwithstanding unusual isotopic fractionation effects (found to be small in the liquid–vapour regime) [25], a crude estimate of the triple-point isotope effect may be obtained as  $\Delta T_{\text{tp}}/T_{\text{tp}} \sim \Delta M/M^3$  (itself proposed in the context of lighter monatomic and diatomic molecules) [26], where  $M$  is the molar mass. In this approach, varying the atomic weight of sulfur between its highest (32.075) and lowest (32.059) naturally-occurring values reported in the literature [27] leads to changes in the  $\text{SF}_6$  triple point temperature of less than  $1 \mu\text{K}$ .

#### 4.11. CSPRT stability

A 10  $\mu\text{K}$  uncertainty contribution due to CSPRT stability is the typical standard deviation of CSPRT temperature readings (calculated from the standard deviation of the F18 resistance bridge readings) after the cell has thermally relaxed into a stable temperature state following a heating pulse. It characterizes the overall level of noise seen in the CSPRT temperature readings.

#### 4.12. Complete uncertainty budget

The complete uncertainty budget for the presently reported sulfur hexafluoride triple point temperature determination on the ITS-90 is summarized in table 2, showing that the combined standard uncertainty for the assigned triple point temperature of 223.555 23 K on the full ITS-90  $e\text{-H}_2\text{-TPW}$  subrange is 0.49 mK. Repeating the same analysis using the Ar-TPW ITS-90 subrange calibration gives an  $\text{SF}_6$  triple point temperature of 223.555 20 K with a combined standard uncertainty of 0.49 mK, showing that the  $\text{SF}_6$  triple point is close enough to the mercury triple point that the inconsistency between ITS-90 subranges is minimal.

If sulfur hexafluoride were assigned a triple point temperature as a defining fixed point of a future revision of the International Temperature Scale, the uncertainty components due to propagated calibration uncertainty and CSPRT non-uniqueness would no longer be relevant to the uncertainty budget, leading to a standard uncertainty of 0.43 mK. This level of measurement realization uncertainty is approximately a factor of two larger than the NRC standard uncertainties for the current ITS-90 defining fixed points listed in table 1.

### 5. Conclusion

Based on a linear fit versus melted fraction  $F$  to an  $\text{SF}_6$  melt plateau, extrapolated to the liquidus point at  $F = 1$ , the triple point of sulfur hexafluoride has been determined to be 223.555 23(49) K ( $k = 1$ ) on the full low-temperature  $e\text{-H}_2\text{-TPW}$  subrange of the ITS-90. This triple point temperature is in excellent agreement with the best previous values reported in the literature [10, 11], but has been determined with considerably smaller uncertainty than those published previously. The high quality of the reported  $\text{SF}_6$  melting curve indicates that the  $\text{SF}_6$  triple point has potential for an expanded role in fixed-point thermometry beyond its current status as a “second quality” secondary reference point [2]. In particular, the triple point of sulfur hexafluoride merits further study (primarily to more deeply explore the effects of chemical impurities) as a promising candidate to be added as a defining fixed point in the next revision of the International Temperature Scale as an alternative to mercury.

### Acknowledgments

The author would like to thank K.D. Hill, A.D.W. Todd, S.N. Dedyulin, W.L. Tew, and M.J. Chojnacky for useful discussions.

## References

- [1] Preston-Thomas H 1990 *Metrologia* **27** 3-10  
Preston-Thomas H 1990 *Metrologia* **27** 107 (erratum)
- [2] Bedford R E, Bonnier G, Maas H and Pavese F 1996 *Metrologia* **33** 133–54
- [3] Hill K D and Steele A G 2005 *Metrologia* **42** 278–88
- [4] Mangum B W, Bloembergen P, Chattle M V, Fellmuth B, Marcarino P and Pokhodun A I 1997 *Metrologia* **34** 427–9
- [5] Hill K D and Steele A G 2003 *AIP Conf. Proc.* **684** 53–8
- [6] Moissan H and Lebeau P 1900 *Compt. Rend.* **130** 865
- [7] Christophorou L G, Olthoff J K and Van Brunt R J 1997 *IEEE Elect. Insul. Mag.* **13** 20–4
- [8] Guder C and Wagner W 2009 *J. Phys. Chem. Ref. Data* **38** 33–94
- [9] Lecoutre C, Guillaument R, Marre S, Garrabos Y, Beysens D and Hahn I 2015 *Phys. Rev. E* **91** 060101(R)
- [10] Blanke W, Klingenberg G and Weiss R 1993 . *PTB-Mitt.* **103** 27–35
- [11] Funke M, Kleinrahn R and Wagner W 2001 *J. Chem. Thermodynamics* **34** 735–54
- [12] Hill K D and Steele A G 2004 *Proc. TEMPMEKO 2004 (Croatia: Cavtat-Dubrovnik, 22–25 June 2004)* **1** pp 295–300
- [13] Steele A G 1997 *The International Seminar on Low Temperature Thermometry and Dynamic Temperature Measurement (Wroclaw, Poland)* ed A Szymrka-Grzebyk pp L48–53
- [14] Hill K D 2002 *Proc. TEMPMEKO 2001* ed B Fellmuth *et al* (Berlin: VDE Verlag) pp 543–8
- [15] Ancsin J 1992 *Metrologia* **29** 71–8
- [16] Hill K D and Fahr M 2011 *Int. J. Thermophys.* **32** 173–88
- [17] Hill K D 2013 *AIP Conf. Proc.* **1552** 198–203
- [18] Ohta T, Yamamuro O and Suga H 1994 *J. Chem. Thermodynamics* **26** 319–31
- [19] Fellmuth B 2013 *AIP Conf. Proc.* **1552** 174–9
- [20] Fellmuth B, Hill K D, Pearse J V, Peruzzi A, Steur P P M and Zhang J 2015 Guide to the Realization of the ITS-90: Chapter 2: Fixed Points: Section 2.1: *Influence of Impurities*, Edition 2015. CCT publications and bibliography: Guidance documents: <http://www.bipm.org/en/committees/cc/cct/publications-cc.html#thermometry-guides>
- [21] Mohr P J, Taylor B N and Newell D B 2015 *The 2014 CODATA Recommended Values of the Fundamental Physical Constants (Web Version 7.0)* available at <http://physics.nist.gov/constants>
- [22] Steele A G, Fellmuth B, Head D I, Hermier Y, Kang K H, Steur P P M and Tew W L 2002 *Metrologia* **39** 551–71
- [23] Kiefe H, Penney R and Clouter M J 1988 *J. Chem. Phys.* **88** 5846–9
- [24] White D R, Ballico M, Chimenti V, Duris S, Filipe E, Ivanova A, Kartal Dogan A, Mendez-Lango E, Meyer C, Pavese F, Peruzzi A, Renaot E, Rudtsch S and Yamazawa K 2014 *Uncertainties in the Realisation of the SPRT Subranges of the ITS-90*, 2014 revision. CCT 24<sup>e</sup> Session, Doc. CCT/08-19-rev2. CCT working documents: 24th meeting (2008): [http://www.bipm.org/cc/CCT/Allowed/24/Uncert\\_CCT-08-19-rev-2014-01-24.pdf](http://www.bipm.org/cc/CCT/Allowed/24/Uncert_CCT-08-19-rev-2014-01-24.pdf)
- [25] Eiler J, Cartigny P, Hofmann A E and Piasecki A 2013 *Geochim. Cosmochim. Acta* **107** 205–19
- [26] Tew W L 2008 *Int. J. Thermophys.* **29** 67–81
- [27] Wieser M E and Coplen T B 2011 *Pure Appl. Chem.* **83** 359–96

**Tables****Table 1.** The uncertainties of the ITS-90 calibration points (in millikelvins) and their influence propagated to the sulfur hexafluoride triple point at 223.555 23 K (in microkelvins).

Fixed point	Uncertainty at the calibration point / mK ( $k = 1$ ) [3, 22]	Uncertainty propagated to 223.555 23 K / $\mu$ K ( $k = 1$ )
Hydrogen triple point	0.2	0.1
17.0373 K (IGT)	0.5	1
20.2734 K (IGT)	0.5	4
Neon triple point	0.2	2
Oxygen triple point	0.2	6
Argon triple point	0.2	11
Mercury triple point	0.2	232
<b>Combined propagated calibration uncertainty</b>		<b>232</b>

**Table 2.** Standard uncertainty of the sulfur hexafluoride triple point determination.

	$\mu\text{K}$
<b>Uncertainty components, Type B</b>	
Chemical impurities	410
Propagated calibration uncertainty	232
Uncertainty propagated from the TPW	80
Hydrostatic pressure	76
CSPRT Type 3 non-uniqueness	53
Determination of fixed point value	27
Static temperature measurement	22
CSPRT self-heating correction	18
Accuracy of resistance bridge ratio	13
Standard resistors	2
Dynamic temperature measurement	1
Isotopic composition	1
<b>Uncertainty components, Type A</b>	
CSPRT stability	10
<b>Combined standard uncertainty</b>	<b>489</b>

## Figures

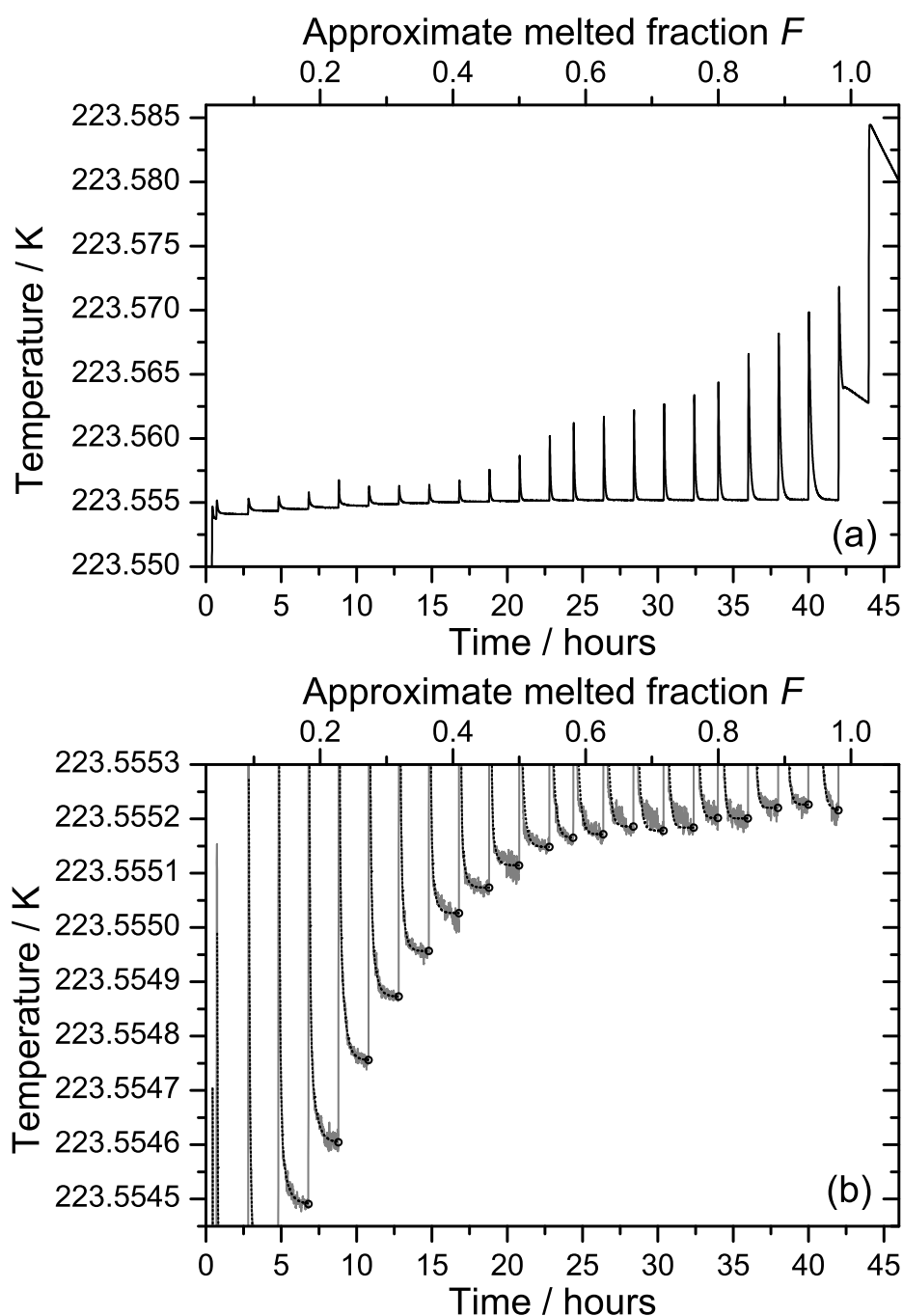


**Figure 1.** Temperature of CSPRT 1876687 measured during the melt of our SF<sub>6</sub> sample. The plotted data has been corrected for thermometer self-heating effects. Each vertical transient corresponds to a 10 J heater pulse, which initially causes a temperature rise in the fixed point cell housing before being absorbed into the SF<sub>6</sub> sample. The dotted lines in panel (b) represent exponential fits to the thermal recovery periods following the heater pulses, and the open symbols represent the asymptotic equilibrium temperatures  $T_{c, \text{equ}}$  obtained from the exponential fits.

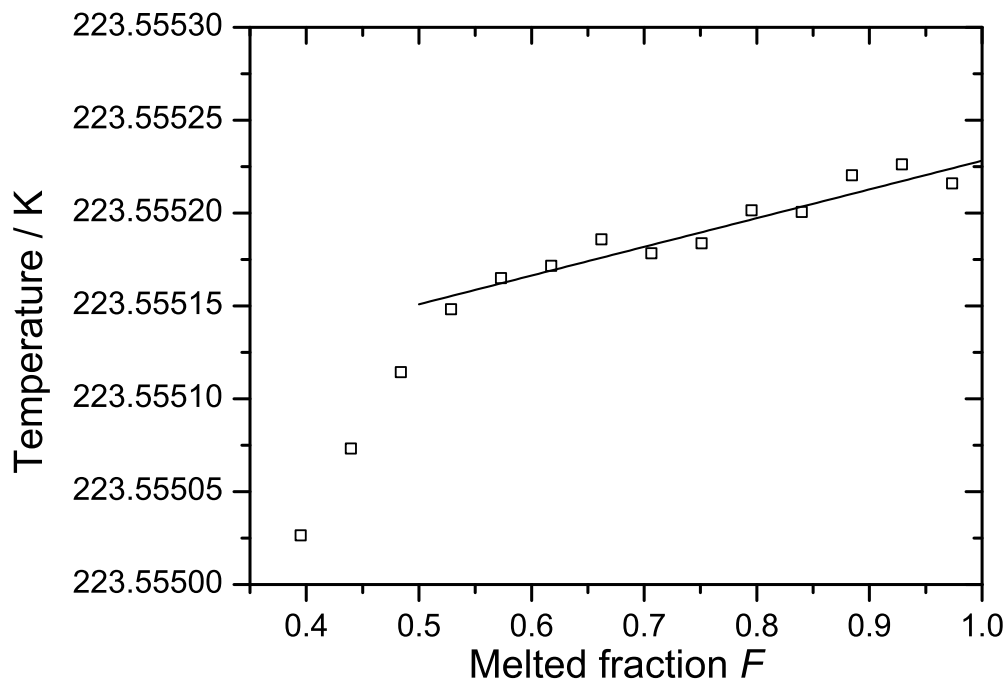


**Figure 2.** Temperature versus melted fraction  $F$  for the  $\text{SF}_6$  melt shown in Figure 1. The open symbols represent the self-heating-corrected asymptotic equilibrium temperatures  $T_{c,\text{equ}}$  obtained from the exponential fits shown in Figure 1 (b). The solid line is a linear fit to the experimental data between 0.53 and 0.84 melted fraction, extrapolated to the liquidus point at  $F = 1$ .